GW and beyond approaches to quasiparticle properties in metals

Marco Cazzaniga*

Università degli Studi di Milano, Physics Department and European Theoretical Spectroscopy Facility (ETSF), via Celoria 16, 20133 Milano, Italy

(Received 24 October 2011; revised manuscript received 9 May 2012; published 13 July 2012)

We perform a comparative study of the performances of some standard approaches within the many-body perturbation theory. We calculate quasiparticle dispersions, lifetimes, and spectral functions of aluminum and sodium. Calculations have been carried out in the *GW* approximation with a plasmon pole model (PPM) or with the contour deformation technique. We also accounted for vertex corrections either only in the screening (replacing the RPA dielectric function with the TDLDA or the Hubbard one) or both in the screening and in the self-energy (using the Del Sole *et al*. local vertex). Results show the failure of the PPM to describe the corrections far from the Fermi energy, as well as its inability to describe quasiparticle lifetimes and spectral functions. Calculations with a more refined screened interaction decrease the bandwidths and the lifetime of the quasiparticles compared with the *GW* as well as inducing tiny modifications in the spectral functions. The inclusion of the vertex also in the self-energy cancels the effects arising from the screening by pushing the results back toward the *GW* ones or even enlarging the differences.

DOI: 10.1103/PhysRevB.86.035120 PACS number(s): 71.10.−w, 71.20.−b, 71.15.Dx, 71.90.+q

I. INTRODUCTION

Starting from good band gaps obtained with the first calculations on bulk Si,[1,2] a wide number of applications (see, e.g., Refs. 3 and 4) consecrated Hedin's *GW* approximation[5,6] as one of the most accurate theories for the description of quasiparticle band structure of weakly correlated systems. Nowadays, applications of the *GW* approximation range over a wide class of materials, yielding good descriptions not only for semiconductors or simple metals, but also for rather complex systems.[7,8]

Quasiparticle energies are not the only quantities which are accessible through a *GW* calculation. The self-energy being a non-Hermitian potential, its eigenvalues are complex, and their imaginary part corresponds to the inverse lifetime of the states due to electronic origin. Such quantities have been investigated for a wide class of materials.[9,10] In the same way the knowledge of the frequency dependence of the self-energy allows the determination of the single-particle spectral functions. A mismatch between theory and experiment (*GW* produces satellites placed at 1.5 times the plasma frequency against one plasma frequency given by measurements)[11,12] has been addressed only thanks to a cumulant expansion[13] or alternative approaches for the evaluation of the single-particle Green function,[14] so that the physics underlying the spectral functions is still the object of investigation.

Improvements in theory development and in computational performances have allowed us to overcome the simplifications of the first applications, despite the fact that some of them are commonly used anyway. For example, self-consistent calculations have been performed,[15,16] sometimes relying on the self-consistent quasiparticle approach.[8,17]

Here we are interested in overcoming the basic approximation of a *GW* approach, which is the neglect of vertex corrections. Some authors have proposed the refinement of many-body calculations by adopting a more accurate screened interaction calculated in the framework of time-dependent density-functional theory (TDDFT). For example, applications are available for homogeneous electron gas (HEG), discussing bandwidths,[18–20] lifetimes,[21] and spectral functions.[22,23] On the contrary, only a limited number of works address realistic systems such as Na[24] and Si.[25]

To account for the vertex also in the self-energy is a more complex task and proposed calculations usually rely on simplified vertices (like the one tested on bulk Si in Refs. 25–27) or addresses the HEG.[28] Only a few authors have discussed the differences arising in the results among the different vertex corrections. They have generally addressed the HEG, by discussing the bandwidths[19,20] or lifetimes.[21] On the contrary, to the best of our knowledge, for realistic systems, only the band gap of silicon has been addressed.[25]

The objective of the present work is to explore the problem, trying to understand the effects on the main quantities which are accessible by many-body calculations and trying to draw general conclusions. With this aim, we perform a systematic study of the performances of some available approaches applied to nearly-free-electron metals such as aluminum and sodium. We focus on the main quantities which are accessible through a non-self-consistent approach, like the quasiparticle dispersion (also discussing the bandwidth problem), finite quasiparticle lifetimes, and spectral functions.

This work is organized as follow: in Sec. II we briefly summarize the theoretical background and the approximations used in the present paper. Then in Sec. III we discuss our results, starting with the quasiparticle dispersion in Sec. III A, moving to the quasiparticle lifetimes in Sec. III B, and concluding with the spectral functions in Sec. III C. We give our conclusions in Sec. IV.

II. TECHNICAL METHODS

A. Theoretical framework

In the present work the many-electron problem is addressed thanks to Hedin's scheme, which is based on the following closed set of five equations:[5,6]

$$G(1,2) = G_0(1,2) + \int G_0(1,3)\Sigma(3,4)G(4,2)\,d3d4, \quad (1)$$

$$\Gamma(1,2;3) = \delta(1,2)\delta(1,3) + \int \frac{\delta\Sigma(1,2)}{\delta G(4,5)} G(4,6)G(7,5)\Gamma(6,7;3)\, d4d5d6d7, \tag{2}$$

$$\chi(1,2) = -i\int G(1,3)G(4,1)\Gamma(3,4;2)\, d3d4, \tag{3}$$

$$W(1,2) = v_C(1,2) + \int v_C(1,3)\chi(3,4)W(4,2)\, d3d4, \tag{4}$$

$$\Sigma(1,2) = i\int G(1,3)W(4,1)\Gamma(3,2;4)\, d3d4\,, \tag{5}$$

where G and G_0 are the exact and Hartree's Green functions, v_C is the bare Coulomb interaction, W is the screened potential, χ is the polarizability, Σ is the self-energy, and Γ is the vertex function. An argument such as" 1" stands for the set of position, time, and spin variables $(\mathbf{r}_1,t_1,\sigma_1)$.

Equations (1)–(5) constitute a formally closed set of equations for the five correlators, which, in principle, one has to solve self-consistently. Starting from the assumptions $\Sigma = 0$ and $G = G_0$, one can solve Eq. (2) to calculate Γ. Its knowledge permits us to invert Eq. (3) to obtain χ, which allows the determination of W thanks to Eq. (4). Then an updated self-energy can be computed thanks to Eq. (5) and a new iteration can start.

It is a standard procedure to avoid a self-consistent solution of Hedin's equation by retaining the first iteration self-energy. In the following we address only this approach to the calculations of the self-energy; a discussion of the effects of self-consistency can be found elsewhere (e.g., in Refs. 15 and 17). The complexity of the equation for the self-energy suggests simplifying the problem further. Because of the theoretical and computational issues involved in the presence of the vertex and in the task of the ω-axis integration, several approaches to the problem have been suggested. In particular, in Sec. II B we introduce those which are tested in this paper. In addition, nowadays, these many-body calculations relies on a DFT ground state which brings the need to account for V_{xc} in the equations.

The knowledge of the self-energy permits the evaluation of several quasiparticle properties. In a one-iteration scheme, quasiparticle energies E_j can be obtained as first-order corrections to the Kohn-Sham (KS) eigenvalues ϵ_j, with respect to the perturbation $(\Sigma - V_{xc})$, and by linearizing the energy dependence of Σ,[1,2]

$$E_j \simeq \epsilon_j + \frac{\langle j|\Sigma(\epsilon_j) - V_{xc}|j\rangle}{1 - \langle j|\frac{\partial\Sigma(\omega)}{\partial\omega}\big|_{\omega=\epsilon_j}|j\rangle}, \tag{6}$$

where $\langle j|$ are the KS eigenstates and the denominator defines the quasiparticle renormalization factor $Z_j = [1 - \langle j|\frac{\partial\Sigma(\omega)}{\partial\omega}|_{\omega=\epsilon_j}|j\rangle]^{-1}$.

The self-energy being a non-Hermitian operator, its eigenvalues will present an imaginary part whose inverse is interpreted as the lifetime of the quasiparticle due to electronic de-excitations. The quasiparticle lifetimes are given by

$$\tau_j^{-1} = 2|\langle j|\mathrm{Im}\Sigma(E_j)|j\rangle| = 2Z_j|\langle j|\mathrm{Im}\Sigma(\epsilon_j)|j\rangle|. \tag{7}$$

For convenience we refer to this approach as full$Z$ even though this is not used in the present paper. In general, the imaginary part of the renormalization factor is considered negligible; therefore the quasiparticle lifetimes are evaluated as[10,29]

$$\tau_j^{-1} = 2\mathrm{Re}Z_j|\langle j|\mathrm{Im}\Sigma(\epsilon_j)|j\rangle|. \tag{8}$$

We refer to this approach as ReZImΣ. A further approximation in the lifetime calculation is the on-mass-shell approximation (OMSA), which comprises the complete neglect of the renormalization factor $(Z_j = 1)$,[30] so that

$$\tau_j^{-1} = 2|\langle j|\mathrm{Im}\Sigma(\epsilon_j)|j\rangle|. \tag{9}$$

In the end it is possible to calculate also the single-particle spectral function,

$$A_j(\omega) = \frac{1}{\pi}\mathrm{Im}\left\{\frac{1}{(\omega-\epsilon_j) - \Sigma_{jj}(\omega)}\right\} = \frac{1}{\pi}\frac{|\mathrm{Im}\Sigma_{jj}(\omega)|}{|\omega - \epsilon_j + V_{xcj} - \mathrm{Re}\Sigma_{jj}(\omega)|^2 + |\mathrm{Im}\Sigma_{jj}(\omega)|^2}, \tag{10}$$

where the presence of the matrix element of V_{xc} accounts, once again, for the fact that the perturbative GW calculation relies on KS eigenstates.

B. Approximations for the self-energy

Different approaches have been proposed to calculate the self-energy. The simplest choice is the complete neglect of the vertex both in the screened interaction and in the self-energy. This approach yields the so-called GW approximation.[5,6] Therefore W reduces to the Coulomb interaction times the random phase approximation (RPA) inverse dielectric function ϵ^{-1} and the equation for the self-energy simplifies to the product of the Green function and the screened interaction:

$$\Sigma(1,2) = iG(1,2)W(2,1). \tag{11}$$

Within the GW approximation further simplifications have been proposed to easily manage the integration required to evaluate the self-energy. Since one bottleneck for the calculation is the evaluation of the dielectric matrix, one often introduces a plasmon pole model (PPM)[1] for its frequency dependency in order to evaluate ϵ^{-1} at only a limited number of frequencies (usually one or two) and to deal analytically with the convolution necessary to evaluate the self-energy. The dielectric function assumes the following analytical expression:

$$\epsilon^{-1}_{\mathbf{GG'}}(\mathbf{q},\omega) = \delta_{\mathbf{GG'}} + \frac{\Omega^2_{\mathbf{GG'}}(\mathbf{q})}{\omega^2 - \tilde{\omega}^2_{\mathbf{GG'}}(\mathbf{q})}. \tag{12}$$

The evaluation of the parameters Ω^2 and $\tilde{\omega}^2$ can be performed in several ways. The first approach proposed was to determine the parameters by imposing the model ϵ^{-1} to match the calculated one at $\omega = 0$ and to fulfill the f-sum rule.[1] In this work we adopt a different scheme based on the evaluation of the dielectric matrix at two frequencies (usually $\omega = 0$ and $\omega = i\omega_P$, where ω_P corresponds to the plasma frequency of that specific material) and use expression (12) to fit the two numerical values.

The PPM is not expected to work properly for states far from the Fermi level or to describe correctly the imaginary

part of the self-energy. Therefore alternative approaches to deal with Eq. (11) have been proposed.[31,32] In particular, in this work we adopt the contour deformation (CD) technique.[32] In this approach the convolution along the real ω axis is moved to an integration along the imaginary axis plus a summation on the poles in the upper-right and bottom-left quadrants.

The GW is a mere approximation for the self-energy which has been found to work accurately. It is desirable anyway to go beyond introducing vertex corrections. One possibility is to move toward a more accurate description of the screened interaction by replacing the RPA ϵ^{-1} with one calculated in the framework of TDDFT (this corresponds to the inclusion of a vertex only in the screened interaction and not in the self-energy).

Older studies of the loss function and the dynamic structure factor demonstrate the time-dependent local-density-approximation (TDLDA)[33] to provide an accurate description for the screening of both semiconductors[34–36] and metals.[37,38] This approximation corresponds to a local and static approximation of the kernel, which is defined as $f_{xc}(\mathbf{r},\mathbf{r}') = \delta(\mathbf{r}-\mathbf{r}')[\mathrm{d}v_{xc}^{\mathrm{LDA}}(\rho(\mathbf{r}))/\mathrm{d}\rho(\mathbf{r})]$. Therefore, in this work we are interested in testing how the results are affected by adopting the TDLDA screening instead of the RPA one (henceforth we refer to this approach as the GW_{LDA}).

The TDLDA f_{xc} is not the only available kernel. A large variety of local-field factors (which are proportional to the TDDFT f_{xc}) has been proposed for the HEG. In this work we choose to perform self-energy calculations adopting the screening obtained within the Hubbard local-field factor[39] (we refer to this approach as the GW_{Hubbard}). This is a local-field factor which includes exchange effects by a model analytical expression: $f_{xc} = -v_c(Q)Q^2/(Q^2+k_F^2)$. A discussion of the accuracy of this local-field factor in the description of the inverse dielectric function of Al and Na can be found in Ref. 38.

To move to more accurate approaches one should include the vertex not only in the calculation of the screened interaction but also in the self-energy. An easy approximation for dealing with this problem has been proposed by Del Sole *et al.*[25] The authors proposed a $GW\Gamma$ approach based, once again, on the TDLDA exchange and correlation kernel f_{xc}. They demonstrate that the inclusion of the TDLDA vertex in Hedin's equations is equivalent to a GW calculation with the screened interaction given by a TDLDA electron-test-charge dielectric function. In this work we perform calculations also with this approach, which is called the $GW\Gamma_{\mathrm{LDA}}$.

In the next section we discuss the difference between the results obtained within these approximations for quasiparticle properties of bulk Al and Na.

C. Computational details

All the calculations presented have been performed with an adapted version of the ABINIT package.[40,41] Calculations have been performed for the experimental lattice parameter, using Troullier-Martins pseudopotentials,[42] and an LDA exchange and correlation functional. We adopted a $14\times14\times14$ k-point mesh, with a smearing temperature of 0.005 Ha and an energy cutoff of 30 Ha for the wave functions and of 15 Ha for the screening and the self-energy, and we included 140 bands in the calculation of both the dielectric matrix and the self-energy. The same set of values has been used for the calculations within the different approximations for the self-energy.

Inclusion of the intraband term in the screened interaction as discussed in Ref. 43 was not possible for the calculations without the PPM, due to the difficulties for performing reliable fits for the lowest real frequencies. Therefore we choose to correct the $\mathbf{G}=\mathbf{G}'=\mathbf{0}$ element of ϵ^{-1} with a Drude-like tail ($\epsilon_{\mathrm{intra}} = 1-\frac{\omega_P^2}{\omega^2}$), evaluating the plasma frequency with the approach described in Ref. 44. In particular, we obtain an intraband plasma frequency ω_P of 12.42 eV for Al and 6.18 eV for Na.

To evaluate the self-energy within the PPM we calculated the screening at $\omega = i15.79$ eV for Al and $\omega = i5.91$ eV for Na. Similarly for the evaluation within the CD technique we calculate the screening over a regular mesh of 10 frequencies on the imaginary axis up to 60.17 eV for Al and 22.53 eV for Na, of 30 real frequencies up to 40.82 eV for Al, and of 52 frequencies up to 27.21 eV for Na.

III. QUASIPARTICLE PROPERTIES

In this section we discuss the results of the calculations on aluminum and sodium with the approaches described in Sec. II B. We discuss the quasiparticle properties, also addressing the bandwidth, the lifetimes, and the spectral function.

A. Quasiparticle energies

The first self-energy calculations on the HEG showed a reduction of the occupied bandwidths with respect of those from DFT,[6] findings confirmed by successive photoemission measurements.[45,46] Consequently, in parallel to the first self-energy calculations on silicon, calculations on nearly-free-electron metals suggested that the use of a TDLDA dielectric function could address the remaining mismatch between GW and experimental bandwidths.[18,24] These findings opened a debate whether the mentioned mismatch in the bandwidth of Na is due to correlation effects beyond GW or, rather, to other problems, such as surface or final-state effects on photoemission measurements.[19,28,47,48] Subsequently, calculations on the HEG with inclusion of vertex corrections also in the self-energy were performed,[19,20] finding bandwidths closer to GW ones than to those calculated with more accurate screened interactions.

The corrections to the KS eigenvalues as defined in Eq. (6) are plotted in Fig. 1 (the results have been aligned by setting the correction at the Fermi level to 0). With the exception of the calculations with the PPM, the general trend is the following: inclusion of the vertex only in the screened interaction increases the magnitude of the corrections more than the GW-CD, while the $GW\Gamma_{\mathrm{LDA}}$ gives the smallest quasiparticle corrections. The results within the GW-PPM are very close to the GW-CD ones in the neighborhood of the Fermi energy, while, as soon as we consider states a few electron volts from the Fermi level, the corrections start to present a different slope.

The PPM constitutes a mere approximation for the real dielectric response, which, for example, does not describe the particle-hole continuum or the plasmon linewidth. In addition, the parameters appearing in Eq. (12) are sensitive to the model

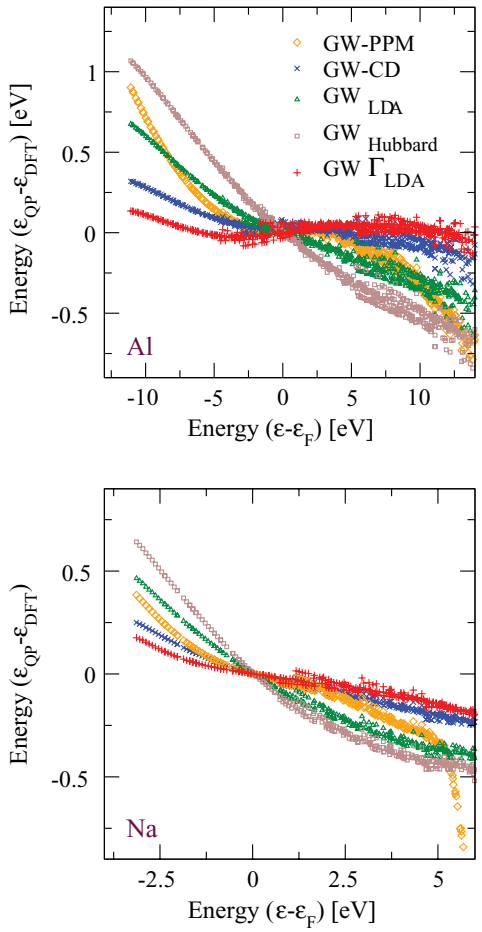

FIG. 1. (Color online) Comparison of quasiparticle corrections calculated within the different approximations dealt with in this work. Corrections are shifted so that they vanish at the Fermi energy. Top, Al; bottom, Na. Calculations with the *GW*-PPM (diamonds), the *GW*-CD (exes), the TDLDA screening (triangles), the Hubbard one (squares), and the Del Sole *et al.* vertex (plus signs).

used. It is a known drawback that, when the PPM is used to evaluate GW corrections, it yields to a poor description of quasiparticle states far from the Fermi level, as confirmed by the present results. In addition, the results of a test adopting the model proposed by Hybertsen and Louie[1] yielded corrections closer to the CD results with respect to the one adopted throughout this work. In the same way, this alternative model induces a shift toward higher energies of the strong deviation of the PPM corrections which can be observed in Na at around 5 eV above the Fermi energy, thus suggesting that this feature is probably a mere artifact of the approximation used.

The bandwidths obtained from the previously discussed GW corrections are listed in Table I. All the approaches produce a reduction in the bandwidth compared to the DFT-LDA one. The GW-PPM produces smaller results than the GW-CD approach, a difference which arises from the expected better description of the bottom valence of this last approach. The introduction of a vertex in the screened interaction produces a further bandwidth reduction with respect to the GW-CD. In particular, for both Al and Na the TDLDA kernel provides a band slightly larger than the Hubbard local-field factor. On the contrary, the inclusion of the vertex also in the self-energy produces, for Na and Al, an increase in the bandwidth with respect to the mere GW-CD calculation.

TABLE I. Occupied bandwidth for aluminum and sodium. Results are compared with old calculations as well as experiments. All energies are in electron volts.

	Al	Na
DFT-LDA	11.706	3.134
GW-PPM	10.192	2.751
GW-CD	10.749	2.887
GW_{LDA}	10.406	2.673
GW_{Hubbard}	10.013	2.498
$GW\Gamma_{\mathrm{LDA}}$	10.946	2.958
Northrup[a] GW_{LDA}(PPM)	10.0	2.52
Cazzaniga[b] PPM	10.03	2.81
Bruneval[c] GW-CD	10.54	
Experiment	10.6 ± 0.2[d]	2.5 ± 0.1[e]
		2.65 ± 0.05[f]

[a]Calculations by Northrup *et al.*[18]
[b]Calculations by Cazzaniga *et al.*[43]
[c]Calculations by Bruneval *et al.*[17]
[d]Experiment by Levinson *et al.*[45]
[e]Experiment by Jensen and Plummer.[46]
[f]Experiment by Lyo and Plummer.[47]

The results of the present work are in substantial agreement with old calculations,[17,18,24,43] while differences can be due to different convergence or methodology to perform the calculations. Our results also show that the inclusion of the vertex in calculations for real metals yields the same conclusions which were drawn for the HEG model.[18–20] Comparing numerical calculations with experiments, the closest results are obtained with the GW-CD for Al and the $\mathrm{GW_{LDA}}$-GW_{Hubbard} for Na. This suggests that none of the approaches discussed here can be addressed as the most accurate. Indeed, there is not a vertex which is closest to the experiment for either material, while more than one result compares favorably with the measurements.

B. Quasiparticle lifetimes

As discussed in Sec. II A, the self-energy being a non-Hermitian operator, the eigenvalues will be complex, and their imaginary part can be interpreted as the inverse lifetime of the quasiparticles. While the imaginary part of the self-energy for the HEG was discussed at the same time as the real one, detailed study of the quasiparticle lifetimes for realistic systems came after the calculations of bandwidths. Two-photon photoemission measurements, providing access to the lifetimes of empty states, were made available only in the 1990s,[49–51] thus raising interest in *ab initio* calculations for realistic systems (for a review of this topic see Refs. 9 and 10). Calculations with inclusion of vertex corrections were discussed for the HEG.[21] In this section we discuss the results for inverse lifetimes.

Figure 2 represents the inverse lifetimes close to the Fermi energy calculated within the approximations discussed in this paper. Of course, the PPM is not expected to be able to describe the lifetime correctly, the model dielectric function

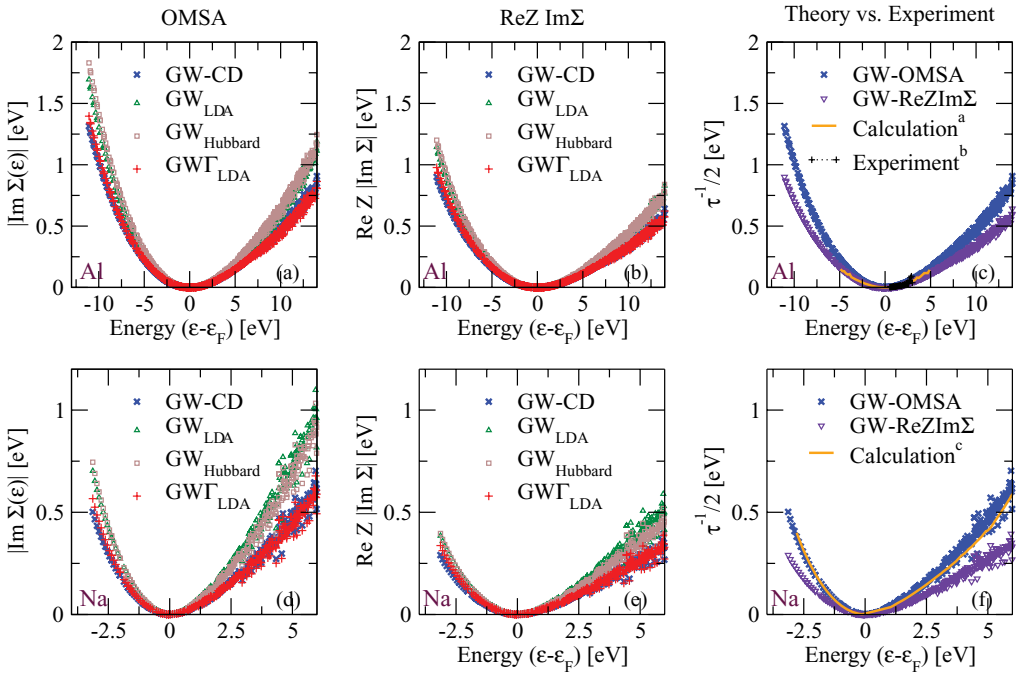

FIG. 2. (Color online) Comparison of quasiparticle lifetimes calculated within the different approximations dealt with in this work. Top row, Al; bottom row, Na. Calculations with the *GW*-CD (exes), the TDLDA screening (triangles), the Hubbard one (squares), and the Del Sole *et al*. vertex (plus). (a, d) Calculations with the OMSA; (b, e) calculations with the ReZImΣ approach; (c, f) comparison of the present calculations with old results and experiment [(a) calculations by Zhukov *et al*.;[52] (b) experiment by Bauer *et al*.;[49] (c) calculations by Dolado *et al*.[30]].

being real. Therefore the discussion refers only to the other approximations.

The results clearly show the expected parabolic behavior around the Fermi energy. In particular, with both the OMSA and the ReZImΣ approach, the GW-CD and the $GW\Gamma_{\mathrm{LDA}}$ approaches give comparable lifetimes in this interval of frequencies for both the metals. In addition, within these approximations the quasiparticle excitations survive longer compared to those calculated including the vertex only in the screened interaction. Comparing the results calculated with the OMSA with those calculated with the ReZImΣ approach, we can observe that the effect of the inclusion of the renormalization factor is an increase in the quasiparticle lifetimes, which can be expected, as $Z_j \leqslant 1$. We found our results to be in substantial agreement with previous calculations for Al[52–57] (not all plotted in Fig. 2). In the same way, GW-OMSA calculations for Na are in substantial agreement with previous calculations.[30] The only available measurements to compare our calculations with are the ones by Bauer *et al*. for Al.[49] In the energy range where measurements have been carried out, the differences between the calculations within the vertices discussed in the present work do not allow us to conclude that one approximation compares better than another one. On the contrary, an improvement in the comparison of theory vs. experiment is achieved when the ReZImΣ approach is adopted instead of the OMSA.

To better visualize the difference in the results we fit the curves with the following equation in the intervals $[-3,3]$ eV for Al and $[-1,1]$ eV for Na:

$$|\mathrm{Im}\Sigma(\epsilon)| \sim \alpha(\epsilon - \epsilon_F)^2. \qquad (13)$$

The resulting coefficients α are listed in Table II. The numbers confirm the increase in ImΣ when a more refined screening is adopted. On the contrary, $GW\Gamma_{\mathrm{LDA}}$ produces results very similar to the GW-CD ones. In the same way, the numbers confirm the increase in the quasiparticle lifetimes when the ReZImΣ approach is adopted. The fit performed for the calculations by Dolado *et al*.[30] is comparable with the present results, while the fit for the results of Zhukov *et al*.[52] is slightly larger than our results.

TABLE II. Fitted coefficients α according to Eq. (13). Fits along the interval $[-3,3]$ eV for Al and $[-1,1]$ eV for Na. Results with the OMSA and with the ReZImΣ approach are compared with fits of old calculations. All values are in eV^{-1}.

	Al	Na
	OMSA	
GW-CD	7.6×10^{-3}	4.3×10^{-2}
GW_{LDA}	9.4×10^{-3}	6.3×10^{-2}
GW_{Hubbard}	9.9×10^{-3}	6.0×10^{-2}
$GW\Gamma_{\mathrm{LDA}}$	7.3×10^{-3}	4.2×10^{-2}
	ReZImΣ	
GW-CD	5.6×10^{-3}	2.7×10^{-2}
GW_{LDA}	6.7×10^{-3}	3.7×10^{-2}
GW_{Hubbard}	7.0×10^{-3}	3.5×10^{-2}
$GW\Gamma_{\mathrm{LDA}}$	5.5×10^{-3}	2.8×10^{-2}
Dolado[a] GW-OMSA		4.6×10^{-2}
Zhukov[b] GW-full$Z$	6.3×10^{-3}	

[a]Calculations by Dolado *et al*.[30]
[b]Calculations by Zhukov *et al*.[52]

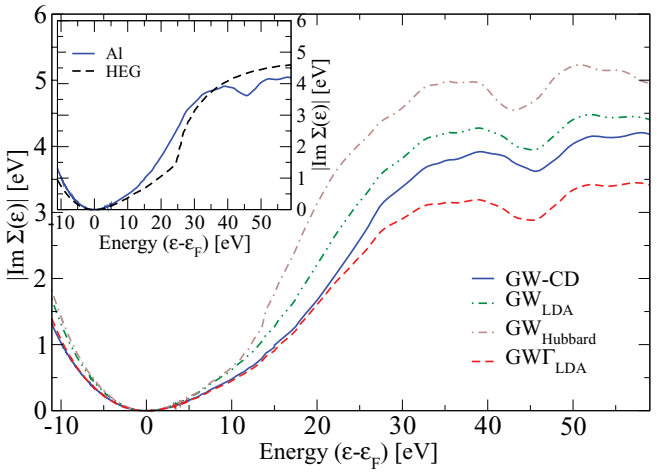

FIG. 3. (Color online) Comparison of the quasiparticle lifetimes of Al calculated with the GW-CD (solid line), the TDLDA screening (dash-dotted line), the Hubbard one (dash-dotted line), and the Del Sole *et al*. vertex (dashed line). Inset: Comparison of GW-CD results for aluminum (solid line) with corresponding results for the HEG from Ref. 58 (dashed line).

We now discuss ImΣ within the OMSA farther from the Fermi energy for aluminum, chosen as the reference. The calculations within the approximations presented in this work show the well-known spreading of the lifetimes for high-energy states.[26,30] To simplify the discussion we choose to retain only the energy dependence, averaging the **k** dependence over the Brillouin zone (BZ) according to

$$\langle \mathrm{Im}\Sigma(\omega)\rangle = \frac{\int_{\mathrm{BZ}} \mathrm{Im}\Sigma(\mathbf{k},\epsilon)\frac{b^2}{(\omega-\epsilon)^2+b^2}d^3k}{\int_{\mathrm{BZ}}\frac{b^2}{(\omega-\epsilon)^2+b^2}d^3k}. \qquad (14)$$

Here ϵ is the energy of the DFT-LDA bands, and b is a parameter to smooth the curve which assumes values from 0.01 near the Fermi energy to 1 for the largest energies. The results are plotted in Fig. 3. Also, for highly unoccupied states the imaginary part of the self-energy is larger when a vertex is included in the screened interaction. In particular, the GW_{Hubbard} approximation produces the smallest lifetimes, followed by the GW_{LDA}, while the $GW\Gamma_{\mathrm{LDA}}$ approximation gives excitations surviving longer. These findings are consistent with the results for the HEG.[21]

More interesting is the comparison with the HEG results (see inset in Fig. 3). It is possible to observe the absence of slope discontinuity in the Al results. This effect is due to the fact that interband transitions widen the plasmon peak in real solids, and consequently, they smooth the energy dependence of the lifetimes.[30] Another difference which can be observed is the small dip at 45 eV present only in ImΣ for Al. This structure is probably a physical effect since it is not washed out by the average procedure, and it can be related to band structure effects since a similar dip is present in the density of states.

C. Spectral functions

The first applications of Hedin's GW approximation to the HEG found the presence of a satellite in the spectral functions.[59–61] In particular, at the bottom of the valence band the satellite was found at around 1.5 ω_P from the main quasiparticle peak (called the plasmaron) and was demonstrated to be induced by a second 0 in $\omega - \epsilon_j + V_{xc\,j} - \mathrm{Re}\Sigma_{jj}(\omega)$. On the contrary, experimental measurements found the satellite at 1 ω_P, as well as a series of satellites.[11,12] Only a few calculations have been carried out on realistic systems, like those performed on Si by Fleszar and Hanke,[26] arriving at the same conclusions as for the HEG. Improved approaches for the description of the satellite rely on a cumulant expansion,[13] as well as alternative approaches for evaluation of the single-particle Green function.[14] In the following we present the calculated spectral functions for Al and Na.

TABLE III. Difference in the energies of the quasiparticle peak E_{QP} and of the satellite E_S for aluminum and sodium at the bottom of the valence band. Calculations performed by detecting the positions of the peaks in the spectral functions in Figs. 4(a) and 4(b). Results in electron volts or in units of ω_P.

	$E_S - E_{QP}$	
	Al	Na
GW-PPM	21.16 eV, 1.41 ω_P	9.24 eV, 1.48 ω_P
GW-CD	21.88 eV, 1.46 ω_P	9.45 eV, 1.52 ω_P
GW_{LDA}	22.18 eV, 1.48 ω_P	9.59 eV, 1.54 ω_P
GW_{Hubbard}	22.18 eV, 1.48 ω_P	9.75 eV, 1.57 ω_P
$GW\Gamma_{\mathrm{LDA}}$	21.60 eV, 1.44 ω_P	9.53 eV, 1.53 ω_P
Aryasetiawan[a]		9.48 eV, 1.52 ω_P

[a]Calculations by Aryasetiawan *et al*.[13]

In Fig. 4 we plot the real and imaginary part of the self-energy and the resulting spectral functions at the bottom of the valence band and for the first unoccupied state at the Γ point for Al and Na. Our GW-CD spectral function at the bottom of the valence band for Na presents the quasiparticle and the satellite peaks at energies in agreement with a previous calculation,[13] but their relative heights present the opposite behavior. Figure 4 shows that the GW-PPM is able to capture only approximately the shape of the self-energy and the spectral function. The main drawbacks can be observed in the spectral functions, where the peak height and width are completely different from the other calculations. The inclusion of the vertex as done in the approaches discussed in the present work produces tiny differences in both the self-energies and the spectral functions, as already observed for the HEG in Refs. 22 and 23. Small shifts of the peaks and modifications of their height and width are present for both the metals and for both the states presented here. Therefore, none of the approximations tested is able to modify the relative position of the peaks to move the calculated spectral function toward a better agreement with measurements.

Since the differences in Fig. 4 do not allow us to clearly detect the differences among the results calculated with the different vertices, we perform a more quantitative analysis of the results calculated at the bottom of the valence band. In particular, in Table III we report the results for the differences in the extracted energies of the quasiparticle peak (E_{QP}) and of the satellite (E_S) both in electron volts and in units of the plasma frequency ω_P. The listed values show in a quantitative way that, within all the approaches addressed here, the satellite

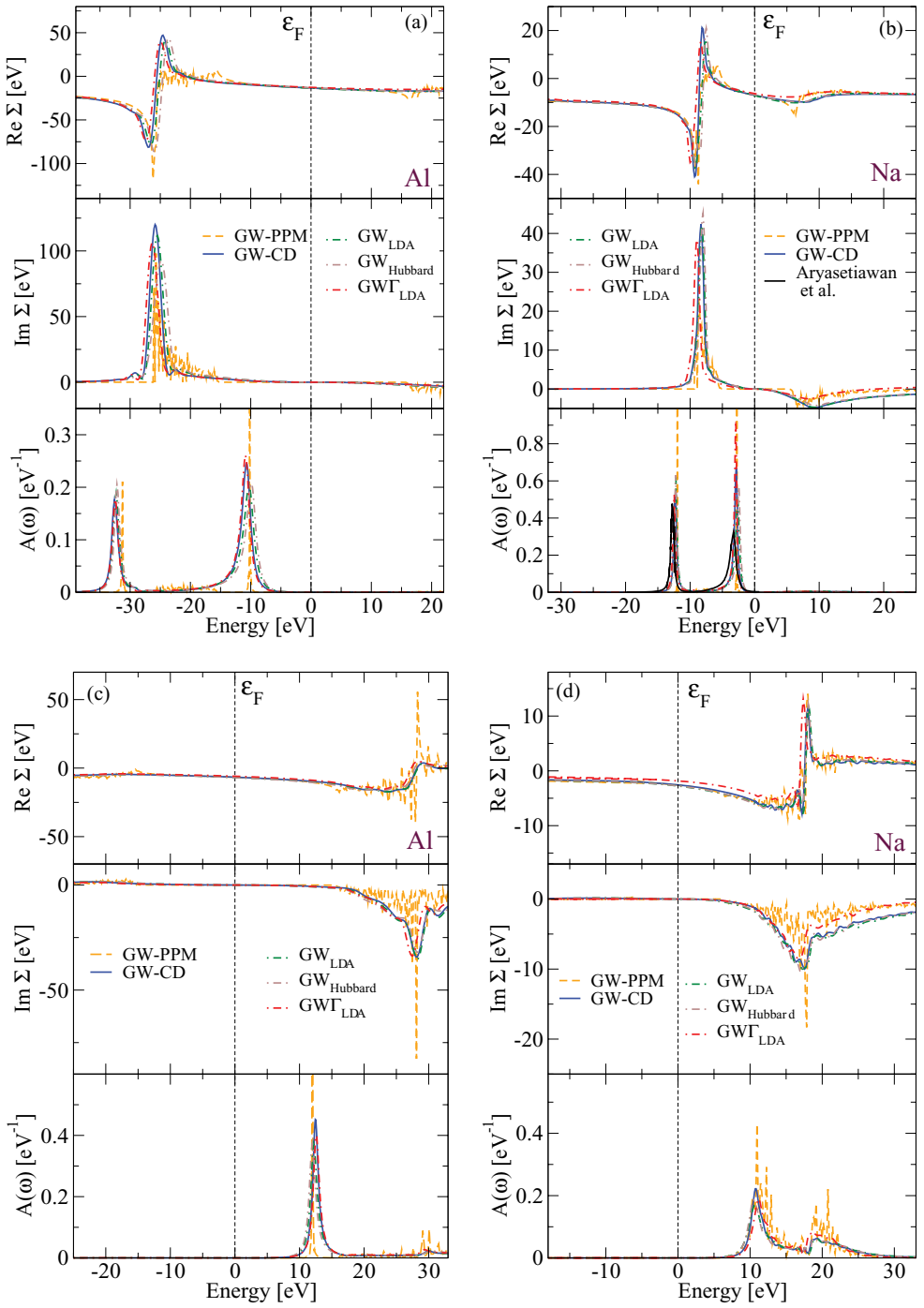

FIG. 4. (Color online) Spectral functions and matrix elements of the self-energy of aluminum and sodium. Comparison of results calculated with the *GW*-PPM (dashed line), the *GW*-CD (solid line), the TDLDA screening (dash-dotted line), the Hubbard one (dash-dotted line), and the Del Sole *et al*. vertex (dash-dotted line). Calculations at the Γ point for the bottom of the valence band [(a) Al and (b) Na] and for the first unoccupied state [(c) Al and (d) Na]. In (b) our results are compared with an old calculation by Aryasetiawan *et al*.[13]

is placed at around 1.5 ω_P from the main quasiparticle peak. The numbers evidence only tiny differences between the discussed approximations. For both metals the PPM produces the smallest distance, while inclusion of the vertex only in the screened interaction increases the distance with respect to the *GW*-CD results. The $GW\Gamma_{\mathrm{LDA}}$ brings the results back toward the *GW*-CD, in relation to which the two metals behave differently: while it brings the satellite closer to the quasiparticle peak in Al, that distance is increased in Na. Alternatively, it is possible to evaluate the same quantity by looking for the zeros of $\omega - \epsilon_j + V_{xc\,j} - \mathrm{Re}\Sigma_{jj}(\omega)$;[59] the results obtained with this approach yield the same considerations drawn before.

In addition to the relative positions of the two peaks, differences between the approximations discussed here can be evidenced by comparing the height and the full width at half-maximum (FWHM) of the quasiparticle peak and

TABLE IV. Height (in eV^{-1}) and FWHM (in eV) of the quasiparticle peak and of the satellite for aluminum and sodium at the bottom of the valence band.

	Al		Na	
	Height	FWHM	Height	FWHM
		Quasiparticle peak		
GW-CD	0.246	1.745	0.669	0.540
GW_{LDA}	0.202	2.068	0.501	0.688
GW_{Hubbard}	0.207	1.956	0.567	0.601
$GW\Gamma_{\mathrm{LDA}}$	0.261	1.677	0.905	0.422
		Satellite		
GW-CD	0.1767	1.233	0.585	0.439
GW_{LDA}	0.189	1.168	0.626	0.446
GW_{Hubbard}	0.205	1.077	0.667	0.415
$GW\Gamma_{\mathrm{LDA}}$	0.1774	1.183	0.524	0.462

of the satellite. The values are listed in Table IV. As for the distance between the two peaks, the differences in the results are small. The general trend for the quasiparticle peak is that, with respect to GW-CD, the $GW\Gamma_{\mathrm{LDA}}$ approach increases the height of the peak and decreases its width, while the other two approximations do the opposite. On the contrary, for the satellite it is more difficult to detect a general trend; while the inclusion of the vertex only in the screened interaction increases the height and decreases the width, the $GW\Gamma_{\mathrm{LDA}}$ produces peaks close to the GW-CD ones. Tiny differences concern an increase in the height of the peak in Al, a decrease in it in Na, and the opposite for the widths.

In conclusion, the small differences among the results calculated with the vertices tested here show that none of the approximations are able to deal with the problem of the position of the satellite. Therefore, to obtain a satisfactory description of the spectral function a more complex approach is required.

IV. CONCLUSIONS

In this work we have performed a comparative study of several many-body approaches to the quasiparticle properties of Al and Na. In particular, we have tested the GW approximation with and without the simplification arising for a PPM for the screening, emphasizing its limitations: we have shown a different behavior of the quasiparticle corrections far from the Fermi energy, the impossibility of describing the imaginary part of the self-energy, and the difficulties in the description of the spectral functions.

We tested the effect of the inclusion of a vertex correction only in the screened interaction by replacing the RPA dielectric function with the TDLDA or the Hubbard one. Results show a decrease in the bandwidth as well as a decrease in the quasiparticle lifetimes. Concerning the spectral functions there are just tiny differences, which reveal a slight breakaway of the satellite from the quasiparticle peak, as well as a small decrease in and widening of the quasiparticle peak, and an opposite behavior of the satellite.

The results are compared with calculations with a local vertex included both in the screening and in the self-energy. In this case we can observe the effects of expected cancelation between the vertex in the dielectric function and the one in the self-energy.[19,20] In particular, quasiparticle bandwidths for Al and Na in the $GW\Gamma_{\mathrm{LDA}}$ become even larger than the GW-CD ones. Similarly, within the same approximation quasiparticles have lifetimes comparable to the GW-CD ones close to the Fermi energy and survive even longer at high energies. In the same way the $GW\Gamma_{\mathrm{LDA}}$ approach has the effect of deleting the small changes in the spectral functions induced by the modified screening interaction, providing results close to the GW-CD ones.

Concerning the performances of the approaches discussed compared to experimental results, we can conclude that none of the tested vertices is able to describe all the quasiparticle properties well, for either metal. Indeed, only small differences were found in the results. In particular, concerning the bandwidths the results closest to experiment are obtained with different vertices for the two metals. For lifetime calculations we found the $\mathrm{Re}Z\mathrm{Im}\Sigma$ approach to work better than the OMSA, but the differences in the results calculated within the first approach do not allow us to conclude that one vertex is preferable. In the end, none of the approaches discussed is able to provide an accurate description of the spectral functions.

ACKNOWLEDGMENTS

This work was supported by the EU's 7th Framework Programme through the European Theoretical Spectroscopy Facility e-I3 Grant No. INFRA-2007-211956. We acknowledge generous supercomputing support from CINECA through the *Calcolo per la Fisica della Materia* initiative and from the CILEA. Useful discussions with F. Bruneval, M. Gatti, M. Giantomassi, V. Olevano, G. Onida, and L. Reining are acknowledged.

*marco.cazzaniga@unimi.it

[1] M. S. Hybertsen and S. G. Louie, Phys. Rev. B **34**, 5390 (1986).

[2] R. W. Godby, M. Schlüter, and L. J. Sham, Phys. Rev. B **37**, 10159 (1988).

[3] W. G. Aulbur, L. Jönsson, and L. W. Wilkins, in *Solid State Physics*, edited by H. Ehrenreich and F. Spaepen (Academic Press, San Diego, CA, 2000), p. 1.

[4] F. Aryasetiawan and O. Gunnarsson, Rep. Prog. Phys. **61**, 237 (1998).

[5] L. Hedin, Phys. Rev. **139**, A796 (1965).

[6] L. Hedin and S. Lundqvist, in *Solid State Physics*, edited by F. Seitz, D. Turnbull, and H. Ehrenreich (Academic Press, New York, 1969), p. 1.

[7] J. Vidal, S. Botti, P. Olsson, J.-F. Guillemoles, and L. Reining, Phys. Rev. Lett. **104**, 056401 (2010).

[8]M. Gatti, F. Bruneval, V. Olevano, and L. Reining, Phys. Rev. Lett. **99**, 266402 (2007).
[9]E. V. Chulkov, A. G. Borisov, J. P. Gauyacq, D. Sánchez-Portal, V. M. Silkin, V. P. Zhukov, and P. M. Echenique, Chem. Rev. **106**, 4160 (2006).
[10]W.-D. Schöne, Progr. Surf. Sci. **82**, 161 (2007).
[11]M. Vos, A. Kheifets, V. Sashin, E. Weigold, M. Usuda, and F. Aryasetiawan, Phys. Rev. B **66**, 155414 (2002).
[12]A. S. Kheifets, V. A. Sashin, M. Vos, E. Weigold, and F. Aryasetiawan, Phys. Rev. B **68**, 233205 (2003).
[13]F. Aryasetiawan, L. Hedin, and K. Karlsson, Phys. Rev. Lett. **77**, 2268 (1996).
[14]M. Guzzo, G. Lani, F. Sottile, P. Romaniello, M. Gatti, J. J. Kas, J. J. Rehr, M. G. Silly, F. Sirotti, and L. Reining, Phys. Rev. Lett. **107**, 166401 (2011).
[15]B. Holm and U. von Barth, Phys. Rev. B **57**, 2108 (1998).
[16]W.-D. Schöne and A. G. Eguiluz, Phys. Rev. Lett. **81**, 1662 (1998).
[17]F. Bruneval, N. Vast, and L. Reining, Phys. Rev. B **74**, 045102 (2006).
[18]J. E. Northrup, M. S. Hybertsen, and S. G. Louie, Phys. Rev. B **39**, 8198 (1989).
[19]G. D. Mahan and B. E. Sernelius, Phys. Rev. Lett. **62**, 2718 (1989).
[20]A. J. Morris, M. Stankovski, K. T. Delaney, P. Rinke, P. García-González, and R. W. Godby, Phys. Rev. B **76**, 155106 (2007).
[21]I. A. Nechaev, I. Y. Sklyadneva, V. M. Silkin, P. M. Echenique, and E. V. Chulkov, Phys. Rev. B **78**, 085113 (2008).
[22]H. O. Frota and G. D. Mahan, Phys. Rev. B **45**, 6243 (1992).
[23]C. Petrillo and F. Sacchetti, Phys. Rev. B **38**, 3834 (1988).
[24]J. E. Northrup, M. S. Hybertsen, and S. G. Louie, Phys. Rev. Lett. **59**, 819 (1987).
[25]R. Del Sole, L. Reining, and R. W. Godby, Phys. Rev. B **49**, 8024 (1994).
[26]A. Fleszar and W. Hanke, Phys. Rev. B **56**, 10228 (1997).
[27]P. A. Bobbert and W. van Haeringen, Phys. Rev. B **49**, 10326 (1994).
[28]H. Yasuhara, S. Yoshinaga, and M. Higuchi, Phys. Rev. Lett. **83**, 3250 (1999).
[29]A. Marini, R. Del Sole, A. Rubio, and G. Onida, Phys. Rev. B **66**, 161104 (2002).
[30]J. S. Dolado, V. M. Silkin, M. A. Cazalilla, A. Rubio, and P. M. Echenique, Phys. Rev. B **64**, 195128 (2001).
[31]A. Marini, G. Onida, and R. Del Sole, Phys. Rev. Lett. **88**, 016403 (2001).
[32]S. Lebègue, B. Arnaud, M. Alouani, and P. E. Bloechl, Phys. Rev. B **67**, 155208 (2003).
[33]E. K. U. Gross and W. Kohn, Phys. Rev. Lett. **55**, 2850 (1985).
[34]M. Ehrnsperger and H. Bross, J. Phys.: Condens. Matter **9**, 1225 (1997).
[35]H.-C. Weissker, J. Serrano, S. Huotari, F. Bruneval, F. Sottile, G. Monaco, M. Krisch, V. Olevano, and L. Reining, Phys. Rev. Lett. **97**, 237602 (2006).
[36]H.-C. Weissker, J. Serrano, S. Huotari, E. Luppi, M. Cazzaniga, F. Bruneval, F. Sottile, G. Monaco, V. Olevano, and L. Reining, Phys. Rev. B **81**, 085104 (2010).
[37]A. A. Quong and A. G. Eguiluz, Phys. Rev. Lett. **70**, 3955 (1993).
[38]M. Cazzaniga, H.-C. Weissker, S. Huotari, T. Pylkkänen, P. Salvestrini, G. Monaco, G. Onida, and L. Reining, Phys. Rev. B **84**, 075109 (2011).
[39]J. Hubbard, Proc. R. Soc. A **243**, 336 (1958).
[40]http://www.abinit.org.
[41]X. Gonze, G. M. Rignanese, M. Verstraete, J. Beuken, Y. Pouillon, R. Caracas, F. Jollet, M. Torrent, G. Zerah, M. Mikami *et al.*, Z. Kristall. **220**, 558 (2005).
[42]N. Troullier and J. L. Martins, Phys. Rev. B **43**, 1993 (1991).
[43]M. Cazzaniga, N. Manini, L. G. Molinari, and G. Onida, Phys. Rev. B **77**, 035117 (2008).
[44]M. Cazzaniga, L. Caramella, N. Manini, and G. Onida, Phys. Rev. B **82**, 035104 (2010).
[45]H. J. Levinson, F. Greuter, and E. W. Plummer, Phys. Rev. B **27**, 727 (1983).
[46]I.-W. Lyo and E. W. Plummer, Phys. Rev. Lett. **60**, 1558 (1988).
[47]E. Jensen and E. W. Plummer, Phys. Rev. Lett. **55**, 1912 (1985).
[48]K. W. K. Shung, Phys. Rev. B **44**, 13112 (1991).
[49]M. Bauer, S. Pawlik, and M. Aeschlimann, Proc. SPIE **3272**, 201 (1998).
[50]C. A. Schmuttenmaer, M. Aeschlimann, H. E. Elsayed-Ali, R. J. D. Miller, D. A. Mantell, J. Cao, and Y. Gao, Phys. Rev. B **50**, 8957 (1994).
[51]T. Hertel, E. Knoesel, M. Wolf, and G. Ertl, Phys. Rev. Lett. **76**, 535 (1996).
[52]V. P. Zhukov and E. V. Chulkov, J. Phys.: Condens. Matter **14**, 1937 (2002).
[53]W.-D. Schöne, R. Keyling, M. Bandić, and W. Ekardt, Phys. Rev. B **60**, 8616 (1999).
[54]I. Campillo, V. M. Silkin, J. M. Pitarke, E. V. Chulkov, A. Rubio, and P. M. Echenique, Phys. Rev. B **61**, 13484 (2000).
[55]F. Ladstädter, U. Hohenester, P. Puschnig, and C. Ambrosch-Draxl, Phys. Rev. B **70**, 235125 (2004).
[56]V. P. Zhukov, E. V. Chulkov, and P. M. Echenique, Phys. Rev. B **72**, 155109 (2005).
[57]I. A. Nechaev, I. Y. Sklyadneva, V. M. Silkin, P. M. Echenique, and E. V. Chulkov, Phys. Rev. B **78**, 085113 (2008).
[58]K. W. K. Shung, B. E. Sernelius, and G. D. Mahan, Phys. Rev. B **36**, 4499 (1987).
[59]B. I. Lundqvist, Phys. Kondens. Materie **6**, 193 (1967).
[60]B. I. Lundqvist, Phys. Kondens. Materie **6**, 206 (1967).
[61]B. I. Lundqvist, Phys. Kondens. Materie **7**, 117 (1967).